20 August 2001

PHYSICS LETTERS A

ELSEVIER

Physics Letters A 287 (2001) 74–80

www.elsevier.com/locate/pla

The circle map dynamics in air bubble formation

A. Tufaile, J.C. Sartorelli *

Instituto de Física, Universidade de São Paulo, Caixa Postal 66318, 05315-970 São Paulo, SP, Brazil

Received 23 March 2001; received in revised form 12 June 2001; accepted 19 June 2001
Communicated by C.R. Doering

Abstract

We studied the air bubbles formation in a submerged nozzle in a water/glycerol solution inside a cylindrical tube, submitted to a sound wave perturbation, whose amplitude is a parameter of control. It was experimentally observed quasiperiodicity, transition from quasiperiodicity to chaos, routes to chaos via period doubling cascade according to the values of $\Omega = f_s/f_b$, where f_s is the sound wave frequency and f_b is the bubbling rate. Our data can be explained by a two-dimensional circle map dynamics. We simulated some bifurcation diagrams as well as some reconstructed attractors with amazing results.

PACS: 05.45.+b
Keywords: Circle map; Bubble dynamics; Arnold tongues

1. Introduction

We studied the air bubble formation dynamics, in a submerged nozzle in a water/glycerol solution inside a cylindrical tube (see Ref. [1] for details), submitted to a sound wave tuned in the air column above the fluid. A small part of the sound wave refracts to the fluid and interacts with the air blowing in the nozzle and changes the bubble formation dynamics. We already have reported [1,2] some dynamical effects of a sound wave in a bubble formation dynamics, such as a flip bifurcation and synchronization, and Hénon-like dynamics. Other features of the bubble oscillator can be found in Refs. [3–7].

In the present Letter we are reporting experimental observations of quasiperiodicity, transition from quasiperiodicity to chaos, period doubling cascade and chaotic behavior, taking the sound wave amplitude as a control parameter. We are showing that air bubble formation in a high viscous liquid follows a circle map dynamics.

The circle map has been used to study two coupled oscillators and to model human heartbeats [8], human hand movements [9], thermoacoustic turbulence [10], and the dynamics of a particle in a rotating liquid [11]. By following the air bubbles displacement through the fluid it should be noticed that when a bubble crosses an observation point above the needle, an amount of fluid is displaced and after the bubble passage through the fluid configuration is restored. So, a bubble train crossing the observation point displaces the fluid with the bubbling frequency f_b, therefore the fluid movement is an oscillatory system and the sound wave tuned to the air column above the liquid represents the other one, whose amplitude (A) corresponds to the coupling strength. In such a way, we related the dynamics of the air bubble formation in a high viscous liquid can follow a circle map dynamics.

* Corresponding author.
E-mail address: sartorelli@if.usp.br (J.C. Sartorelli).

0375-9601/01/$ – see front matter
PII: S0375-9601(01)00460-1

2. The two-dimensional circle map

The two-dimensional circle map is given by [12]

$$x_{n+1} = x_n + \Omega - \frac{K}{2\pi}\sin(2\pi x_n) + by_n \pmod 1,$$
$$y_{n+1} = by_n - \frac{K}{2\pi}\sin(2\pi x_n), \qquad (1)$$

where Ω is the frequency ratio of the uncoupled oscillators, b is an adjustable parameter corresponding to a dumping constant related to contraction of the phase space, and K is the coupling strength which was used as a control parameter. The y_n vs. K diagram bifurcations as well as the first return maps y_{n+1} vs. y_n were used to simulate our experimental data.

3. Experimental apparatus

The air bubble formation experimental apparatus is shown in Fig. 1. The bubbles are generated by injecting air under constant flow rate conditions through a metallic nozzle submerged in a viscous fluid column, and the air flux can be set up by the opening of a needle valve. The dimensions of the cylindrical tube are 53 mm in diameter and 70 cm in height, and the nozzle inner diameter is 0.72 mm. The fluid viscosity can be changed by varying the glycerol concentration η ($(1-\eta)$ water $+\ \eta$ glycerol). We changed the bubble formation dynamics applying a sound wave with a loudspeaker placed at the top of the tube. The sound wave was tuned to the fundamental frequency ($f_s = 150$ Hz) of the air column above the fluid, and the wave amplitude A was driven by a function generator. All the measurements were done at room temperature with $\eta = 0.8$.

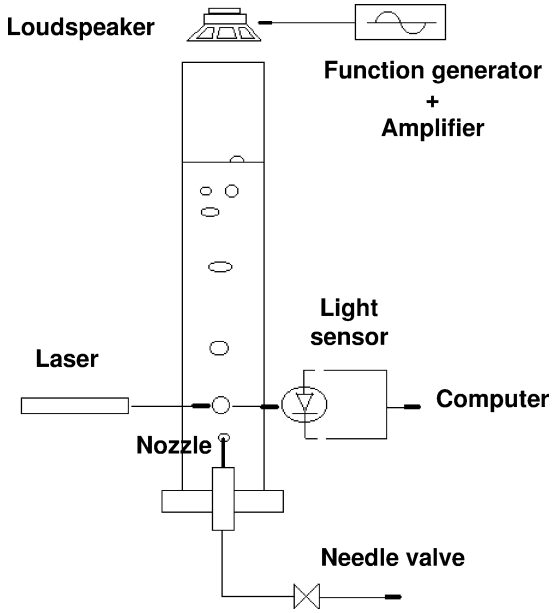

Fig. 1. Diagram of the experimental apparatus.

The detection system is the same as the one in the dripping faucet experiment [13,14]. A horizontal He–Ne laser beam, focused on a photodiode, is placed a little above the nozzle. The delay times between successive bubbles were measured with a time circuitry inserted in a PC slot, with a time resolution equals to 1 μs. The input signals are voltage pulses induced in a resistor by the scattering of a laser beam focused on a photodiode in series with the resistor. The width of pulse is the time interval t_n (n is the bubble number), and the time delay between two pulses is the crossing time (dt_n) of a bubble through the laser beam, so that the total time interval is $T_n = t_n + dt_n$. The bubbling rate is calculated as $f = 1/\langle T\rangle$, where $\langle T\rangle$ is the mean time between successive bubbles.

We changed the bubbling behavior by applying a sound wave with a loudspeaker placed at the top of the tube. The sound wave was tuned to the fundamental frequency ($f_s = 150$ Hz) of the air column above the fluid, and the wave amplitude A was used as control parameter and it is driven by a function generator. All the measurements were done at room temperature.

4. Results and discussion

To obtain an experimental bifurcation diagram, firstly, with no sound wave, we chose a periodic bubbling with $f_b = 1/T_0$. After then, we turned on the function generator and the sound wave amplitude A was increased continuously.

In Fig. 2(a) it is shown an experimental bifurcation diagram T_n vs. A for a bubbling rate of $f_b = 39.37$ bubbles/s, and $\Omega = f_s/f_b = 3.81$, and in Fig. 2(b) a circle map bifurcation diagram y_n vs. K calculated with same value of Ω and $b = 0.1$ [2,15]. There are some similarities between both diagrams. For $K = 0$ and $A = 0$, from the respective period one

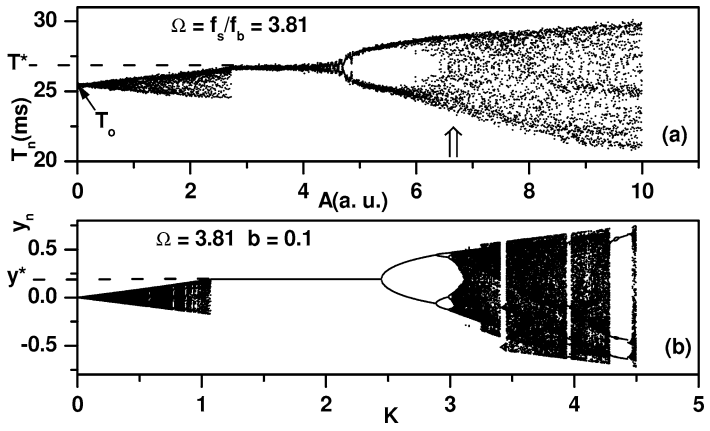

Fig. 2. (a) Experimental bifurcation diagram, T_n vs. A, with the sound wave amplitude as control parameter. $\Omega = f_s/f_b = f_s T_0 = 3.81$, with T_0 obtained with $A = 0$. (b) Bifurcation diagram y_n vs. K, with the same value of Ω and $b = 0.1$. In both cases we can observe the quasiperiodic region (triangle shaped band) and a period doubling cascade. The fixed points ($y^* > 0$ and $T^* > T_0$) are tangent to the upper boundary of the end of the quasiperiodic region. The experimental fixed point is $T^* = 26.7 \pm 0.1$ ms.

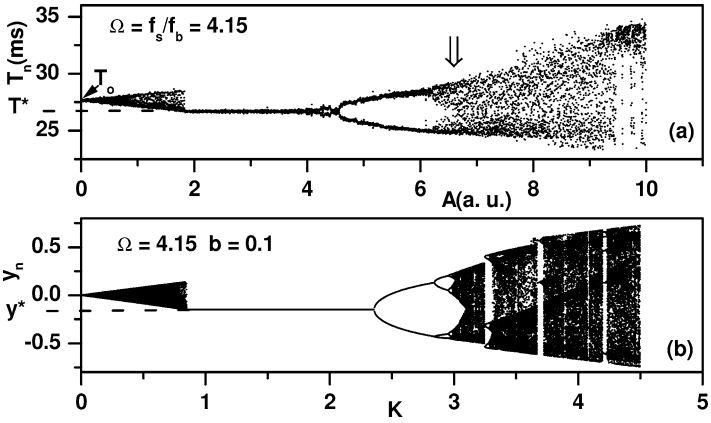

Fig. 3. The same of Fig. 2, with $\Omega = 4.15$. It should be noted the change of the relative position of the fixed points ($y^* < 0$ and $T^* < T_0$) when compared with the respective positions shown in Fig. 2. The dashed lines corresponds to unstable fixed points. The experimental fixed point is $T^* = 26.7 \pm 0.1$ ms.

behavior, $y = 0$ and $T = T_0$, as we increase the control parameter a quasiperiodic region takes place, followed by a chaotic region ($K \sim 1$), and after that the fixed points (y^* and T^*, respectively) suddenly become stable at $K^* \approx 1.07$ and $A^* \approx 2.7$, respectively. It should be noted that these fixed points are tangent to the upper boundary at the end of the triangle shaped band ($y^* > 0$ and $T^* > T_0$) and they continue stable until $K^* \approx 2.44$ and $A^* \approx 4.7$, when the routes to chaos via period doubling start. Consequently, the results are suggesting that the bubble formation can be explained by the circle map dynamics, where the coupling strength is the sound wave amplitude and the frequency ratio of the two uncoupled oscillators is given by the ratio of the sound wave frequency and the bubbling rate, $\Omega = f_s/f_b$.

To supplement this assumption we looked for more detailed similarities. The fixed point in the circle map is given by $y^* = \text{Integer}(\Omega + 0.5) - \Omega$. If we choose a Ω value such as $\text{Integer}(\Omega + 0.5) < \Omega$ the fixed point is negative, and it is located at the lower boundary of the quasiperiodic band, as for the case of $\Omega = 4.15$ and $y^* = -0.15$, as shown in Fig. 3(b). Therefore, we set up the bubbling rate to

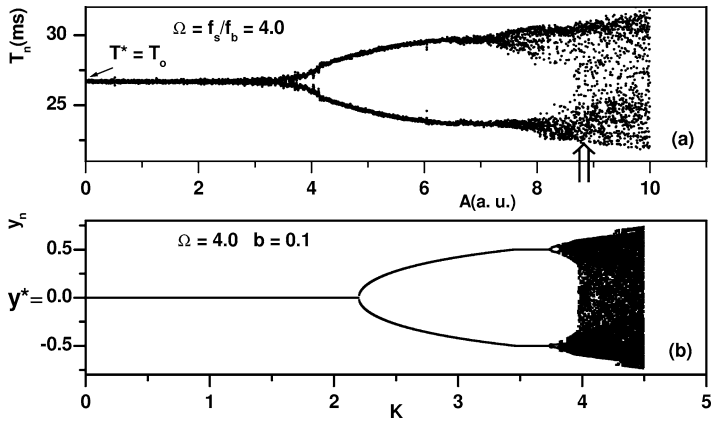

Fig. 4. The same of Fig. 2, with $\Omega = 4.0$. Now there is no quasiperiodic region and $y^* = 0$ and $T^* = T_0$ are stable fixed points. The experimental fixed point is $T^* = 26.66 \pm 0.07$ ms.

36.14 bubbles/s to get the same value of $\Omega = 4.15$, and the experimental bifurcation diagram is shown in Fig. 3(a). Again, the same similarities described above are obtained. The fixed point y^* (T^*) becomes stable at $K^* \approx 0.85$ ($A^* \approx 1.8$) and the period doubling cascade starts at $K^* \approx 2.36$ ($A^* \approx 4.5$). As we can see the experimental fixed point ($T^* < T_0$) is also tangent to the lower boundary of the triangle shaped quasiperiodic region. A similar behavior for a lesser viscous fluid ($\eta = 2/3$) can be followed in the sequence of attractors shown in Fig. 6 of Ref. [1].

Setting up the bubbling rate to $f_b = 37.50$ bubbles/s, so $\Omega = 4.0$, there is no quasiperiodic region in both bifurcation diagrams as shown in Fig. 4. The fixed point $y^* = 0$ ($T^* = T_0$) is stable until $K^* \approx 2.2$ ($A^* \approx 3.7$), and the system evolves directly to the period doubling cascade.

We can divide the system evolution in two regions: an initial region, related to the quasiperiodic behavior ($K \lesssim 1$), and the period doubling route to chaos region ($K \gg 1$).

For the first region, we have sketched a few Arnold tongues shown as shaded areas in Fig. 5 obtained with the unidimensional circle map ($b = 0$) [17] as an approximation to the less dissipative circle map with $b = 0.1$. For a fixed value of $\Omega \pmod 1 \neq 0$ the system evolves in a quasiperiodic region, represented by the vertical dotted arrows, until they find the fixed point given by $y^* \approx K^*/2\pi(1 - b)$, represented by the closed circles. Therefore, the shaped triangular regions, shown in Figs. 2 and 3, correspond to a dynamics related to a torus T^2 evolution. In Fig. 2 we have $K^* \approx 1.07$, for $K > 1$ the Arnold tongues overlap [16], and chaotic bands appear. Therefore, it is observed a torus break up by a transition from quasiperiodicity to chaos. Since for $K < 1$ there are no tongues overlapping, so there is no torus break up for $K^* \approx 0.85$, as it is shown in Fig. 3. For $\Omega \pmod 1 = 0$, as in the case of $\Omega = 4.0$ shown in Fig. 4, the fixed point does not depend on K, as shown by the vertical arrow at $\Omega \pmod 1 = 0$.

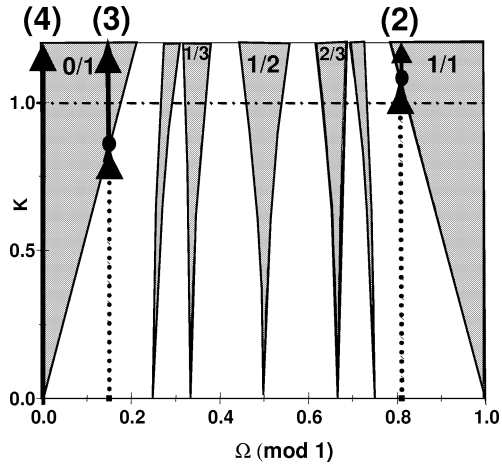

Fig. 5. Some Arnold tongues. The numbers at the top correspond to the data shown in the respective figure. The overlapping of the tongues for $K > 1$ are not drawn.

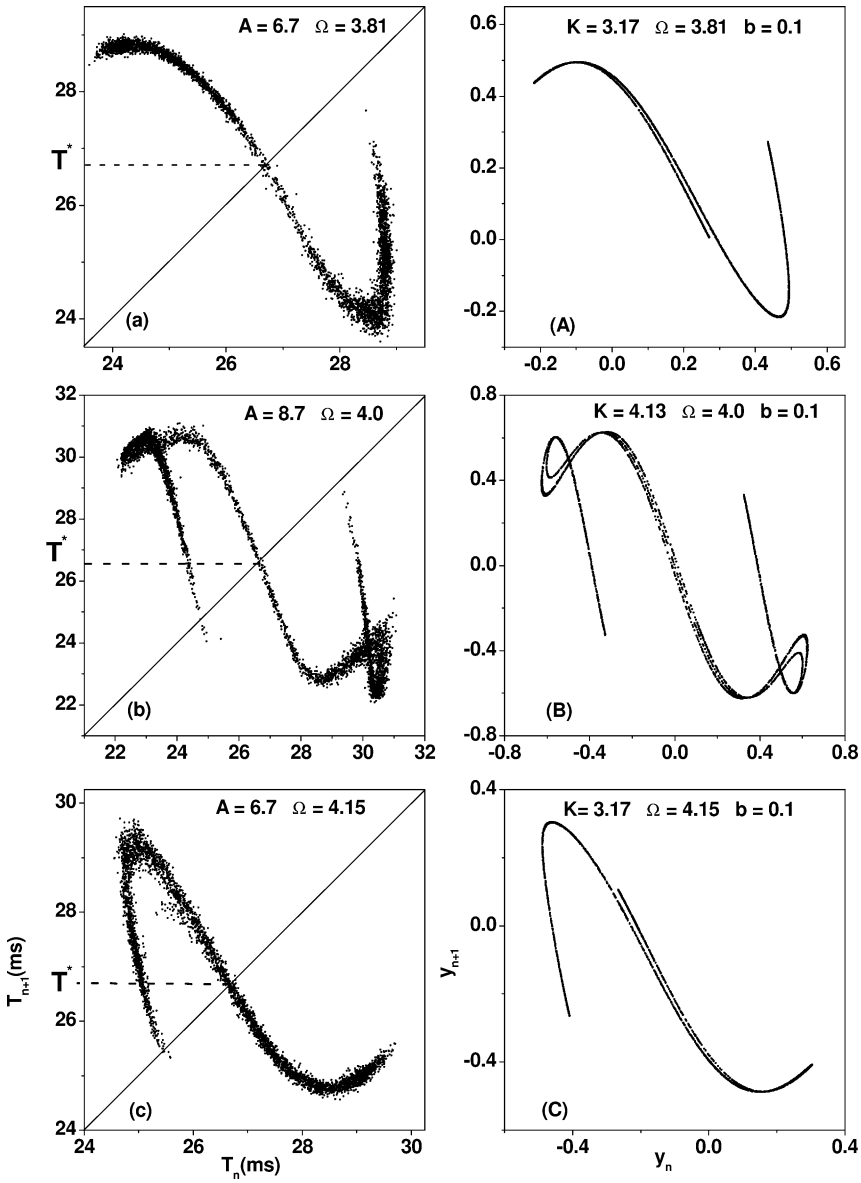

Fig. 6. Left column: some experimental attractors; right column: respective simulation with the circle map. The saddle points are given by the crossing of the lines and the attractors. In all cases $T^* = 26.7$ ms.

To reinforce that the air bubbles formation dynamics is well described by the dissipative two-dimensional circle map, we reconstructed some attractors for $K \gg 1$ using first return maps T_{n+1} vs. T_n. The open vertical arrows in Figs. 2(a), 3(a) and 4(a) indicate approximately the value of the experimental control parameter for the reconstructions shown in Fig. 6, at left column we have the experimental maps T_{n+1} vs. T_n. Each experimental attractor is well simulated by the circle map y_{n+1}vs. y_n with the same Ω value, as it is shown in the right column of Fig. 4.

By rotating 180 degrees the attractor shown in Fig. 6(a) we have obtained a very similar profile of the attractor shown in Fig. 6(c). Due to the symmetry

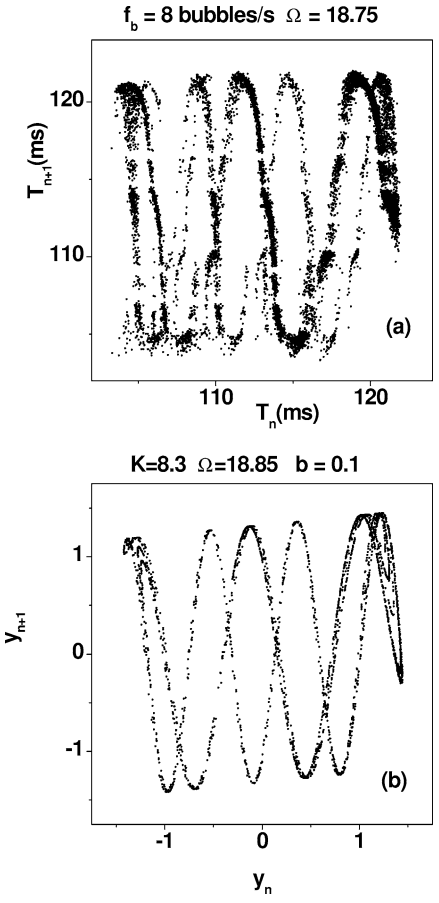

Fig. 7. (a) Experimental attractor obtained at 8 bubbles/s. (b) The simulation with the circle map.

axis at $\Omega = 0.5$ of the Arnold tongues diagram (see Fig. 5), and as $0.15 \sim 1 - 0.81$, both attractors present similar stretching and folding characteristics [2]. The attractor shown in Fig. 6(b) is symmetrically divided by the diagonal line due to the cyclical properties of the Arnold tongues given by Ω (mod 1).

In each attractor we can find the fixed point by the crossing of the diagonal line with the attractor. In this way we found $T^* = 26.7$ ms for the three cases, that is the same value obtained with the bifurcation diagrams shown in Figs. 2(a), 3(a) and 4(a). For these high values of K the fixed points are unstable orbits corresponding to saddle points [1,2], with unstable manifolds tangent to the attractor.

Even more complex experimental attractor can be well simulated, as the one obtained at higher sound wave amplitude, as shown in Fig. 7(a). In this case we set up the bubbling rate to 8 bubbles/s, so $\Omega = 18.75$, and the corresponding simulation with the circle map with $\Omega = 18.85$ and $b = 0.1$ is shown in Fig. 7(b).

5. Conclusion

In conclusion, for $\eta > 3/5$, the two coupled oscillators given by the fluid movement and the sound wave have presented features such as quasiperiodicity, transition from quasiperiodic to chaotic behavior, period doubling cascade, and chaos by varying the amplitude of a sound wave that can be interpreted with the circle map dynamics. In addition, for low coupling we analyzed the data by using Arnold tongues diagram, for three values of the frequencies ratio $\Omega = f_s/f_b$, where f_s is the sound frequency. For high coupling the profiles of the experimental first return maps also reinforced our assumption that the air bubble formation follows a dissipative circle map dynamics.

Acknowledgements

This work was partially supported by Brazilian agencies FAPESP, CNPq, and FINEP. Acknowledgments to M.B. Reyes and M.S. Baptista for the helpful suggestions.

References

[1] A. Tufaile, J.C. Sartorelli, Physica A 275 (2000) 336.
[2] A. Tufaile, J.C. Sartorelli, Phys. Lett. A 275 (2000) 211.
[3] W. Lauterborn, U. Parlitz, J. Acoust. Soc. Am. 84 (1988) 1975.
[4] D.J. Tritton, C. Edgell, Phys. Fluids A 5 (1993) 503.
[5] L.J. Mittoni, M.P. Schwarz, R.D. La Nauze, Phys. Fluids 7 (1995) 891.
[6] H.Z. Li, Y. Mouline, L. Choplin, N. Midoux, Int. J. Multiphase Flow 23 (1997) 173.
[7] M.C. Ruzicka, J. Drahos, J. Zahradnik, N. Thomas, Int. J. Multiphase Flow 23 (1997) 671.
[8] Y. He, R. Chi, N. He, Phys. Lett. A 170 (1992) 29.
[9] H. Haken, C.E. Peper, P.J. Beek, A. Daffershofer, Physica D 90 (1996) 179.
[10] T. Yazaki, Phys. Rev. E 43 (1993) 1806.
[11] M. Piva, A. Calvo, J.E. Wesfreid, J. Phys. D: Appl. Phys. 33 (2000) 1431.
[12] J. Argyris, G. Faust, M. Haase, An Exploration of Chaos, Elsevier, Amsterdam, 1994.

[13] J.C. Sartorelli, W.M. Gonçalves, R.D. Pinto, Phys. Rev. E 49 (1994) 3963.
[14] A. Tufaile, R.D. Pinto, W.M. Gonçalves, J.C. Sartorelli, Phys. Lett. A 255 (1999) 58.
[15] Since the $|\det(J_{CM})| = |\det(J_{HM})| = b$, where J_{CM} (J_{HM}) is the Jacobian of the circle map (Hénon map), we kept the same value $b = 0.1$ used to emulate Hénon-like attractors in Ref. [2].
[16] See color plate I in Ref. [12, p. 397].
[17] Hao Bai-Lin, Elementary Symbolic Dynamics, World Scientific, Singapore, 1989.